Aerodynamic Characteristics of an Axisymmetric Body Undergoing a Uniform Pitching Motion

L.H. Smith*
Naval Weapons Center, China Lake, Calif.

and

R.H. Nunn†
Naval Postgraduate School, Monterey, Calif.

An experimental investigation was conducted to determine the effect of a uniform pitching motion on a slender axisymmetric body while undergoing large excursions in angle of attack. Force and moment measurements were obtained for a slender tangent-ogive/cylindrical body over a range of Reynolds numbers from 5×10^4 to 1.4×10^5 while varying the angle of attack from zero to 90° and the pitch rate between zero and 281°/sec. Smoke flow visualization studies were used as an aid in assessing wake vortex transitions. The results of the investigation show that there is an increment of normal force directly attributable to the uniform pitching motion. The incremental increase in the normal force is sufficient to cause significant errors in calculating body damping derivatives from static force measurements. Distinct wake vortex transitions at approximately 20, 50, and 65° were observed. The effect of a uniform pitching motion shifts the angle of attack at which these wake vortex transitions occur, and can reduce the abruptness of those transitions.

Nomenclature

d = maximum body diameter
Re = $V_0 d/\nu$
t = time
V_0 = freestream velocity
x = axial coordinate
α = angle of attack
$\dot{\alpha}$ = rate of change of angle of attack
ν = kinematic viscosity

Introduction

CERTAIN evolving tactical missile missions require extreme flight agility to accomplish large and rapid heading changes. Such requirements have prompted an interest in the aerodynamic loading of slender missile configurations at large angles of attack and while undergoing rapid pitching through large excursions in angle of attack. A considerable amount of recent research has been directed toward understanding the static aerodynamics of slender bodies of revolution at moderate and high angles of attack. These efforts have revealed that the flow on the leeside of these bodies is characterized by a vortex system that changes with increasing angle of attack from a steady symmetric pair of rolled-up vortex sheets to steady asymmetric shedding of discrete vortices and, finally, at large angles of attack, to an unsteady asymmetric arrangement. Associated with these changing wake vortex patterns are significant yawing forces and moments, which can be larger than the control moments produced by the deflection of conventional control devices. These body generated forces and moments or the interference of the trailing vortices with wings and tails can have a dominant effect on the maneuvering characteristics of a missile.

Presented as Paper 75-838 at the AIAA Fluid and Plasma Dynamics Conference, Hartford, Conn., June 16-18, 1975; submitted July 14, 1975; revision received November 6, 1975.

Index categories: Jets, Wakes, and Viscid-Inviscid Flow Interactions; Nonsteady Aerodynamics.

*Consultant, Conventional Weapons Division. Member AIAA.

†Associate Professor, Department of Mechanical Engineering. Member AIAA.

Emphasis of the present experimental investigation has been placed upon a study to 1) determine the dependence of the aerodynamic loading upon a uniform angular velocity in pitch and 2) identify specific transition regions in the wake vortex pattern and the subsequent alteration of those patterns caused by the rotation. It is realized that for full-scale vehicles in flight there exists the possibility of coupling between the shedding of the wake vortices and the translational motion of the missile. Hence, the results of a wind tunnel investigation using a model, the movement of which is restrained by its mounting system, may not be directly applicable to full-scale vehicles. However, the effects on the wake vortex configuration of certain variables such as pitch rate and Reynolds number may indicate significant trends.

Nature of the Problem

As a body of revolution is exposed to an increasing angle of attack, the flow on its leeward side separates and rolls up to form vortices. Under these conditions, normal force and pitching moment can no longer be predicted by slender body theory. For angles of attack less than approximately 20° (depending on the crossflow Reynolds number) two symmetric vortices form. For larger angles of attack, discrete vortices grow asymmetrically and break away or shed from the leeward side, at first in a spatially periodic manner, while at the higher angles the shedding becomes unsteady.

Analyses of the flow about inclined bodies of revolution have been presented by numerous investigators, incorporating varying degrees of rigor. Almost exclusively these analyses have used the impulsive flow analogy proposed by Allen and Perkins.[1] This analogy assumes that the crossflow is swept down the length of the body at a rate $V_0\cos\alpha$. At each axial station the flowfield is taken to be analogous to the flow about a cylinder in crossflow, whose radius is equal to the body radius at that axial station. The developing (with axial position) crossflow is thus similar to the flow about a cylinder impulsively set in motion from rest. The validity of the impulsive flow analogy depends upon crossflow independence; that is, the viscous flow across the cylinder may be treated independently of the flow along the cylinder. This is only strictly true for laminar boundary layers.

The crossflow Reynolds number at any particular axial station depends upon the angle of attack and the body diameter at that station. Thus, at a specific angle of attack the flow as viewed in crossflow planes develops with increasing crossflow Reynolds number along the nose section, reaching a constant maximum value at the junction of the nose and the afterbody. Near the apex of the nose the crossflow Reynolds number is very low (small body diameter), so that the viscous action is large in comparison to the inertia of the fluid and separation does not occur. As the crossflow Reynolds number increases with increasing axial position, a symmetric vortex pair is formed. At still higher crossflow Reynolds numbers alternate detachment of the vortices on the leeward side of the body takes place, and so on. For a given angle of attack and freestream Reynolds number the crossflow Reynolds number achieves its maximum value along the afterbody. It is the maximum value of the crossflow Reynolds number that determines the final stage of vortex development along the body.

The qualitative models and the methods of analysis range from engineering calculations for determining normal forces and pitching moments,[2-5] to detailed flowfield descriptions which provide information on the separation of the boundary-layer fluid and the growth and detachment of the vortices.[6-10] The prediction of yaw forces, which arise from the asymmetries in the vortex wake, is only achieved using the more complete detailed flowfield descriptions. The technique most commonly used in formulating the more complete flowfield descriptions is the impulsive flow analogy. Use of the analogy reduces the three-dimensional problem to a two-dimensional axially varying (time and axial position are related by $t=x/V_0\cos\alpha$) analysis. Further, the viscous and the potential flow contributions are treated independently and then superimposed.

Concentrating on a potential flow description of the vortex wake, the static forces developed for either the symmetric or spatially periodic asymmetric vortex configurations can be calculated provided the strengths and positions of the wake vortices can be described. The strengths and positions of the vortices are determined by requiring the force on each vortex to balance the force on its feeding sheet, and by specifying that the separation points be stagnation points of the crossflow.

In order to estimate what the effect of a uniform pitching motion might be on an inclined body of revolution, consider the components of the velocity in the crossflow planes. As shown in Fig. 1, the crossflow velocity is composed of two components, the normal velocity caused by the angle of attack and the normal velocity caused by the angular velocity. When these two components of crossflow velocity are added they yield a nonuniform velocity distribution along the length of the body. Since the angle of attack is a function of time, the nonuniform velocity distribution along the body will be unsteady.

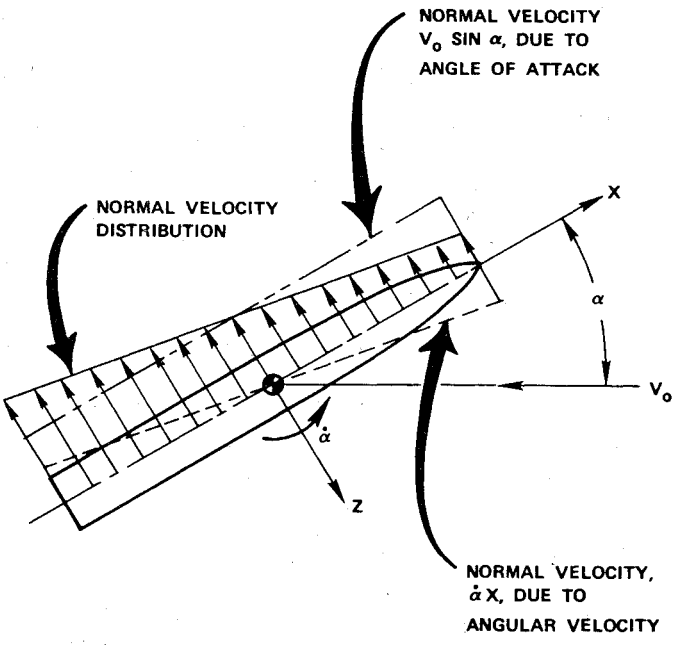

Fig. 1 Velocity distribution on an inclined body of revolution while undergoing a uniform pitching motion.

Note that the choice of the axial station about which the body is rotated will directly influence the velocity in the crossflow planes, therefore, the body forces developed during uniform pitching will be dependent upon the location of the axis of rotation. If the axis of rotation were placed at the apex of the nose, the effect of the angular motion would be to increase the normal velocity at all axial positions and increasing the normal force with increasing angular velocity. This result was demonstrated in an investigation conducted by Sarpkaya[11] for a rotating flat plate in a uniform flow. Glauert[12] obtained a similar result in an analysis of the lift and pitching moment on an airfoil caused by a uniform angular velocity of pitch.

Experimental Apparatus

The experimental phase of this investigation was carried out in a low-turbulence subsonic wind-tunnel facility especially designed and instrumented for this purpose. The aerodynamic forces and moments were measured using a six-component floating frame TASK internal strain gage balance. A single model was used for all of the experiments. The model was a right circular cylinder with a three-caliber tangent-ogive nose and an overall length to diameter ratio of 15 to 1. The model was rotated at a constant angular velocity about an axis normal to the axis of symmetry in an otherwise uniform flow. The axis of rotation was located at the center of gravity of an assumed homogeneous body, or 8.179 diam aft of the apex of the nose.

Experiments were conducted at freestream Reynolds numbers of 5×10^4, 8×10^4, and 1.4×10^5, based on the maximum body diameter. The angle of attack was varied between zero and 90° and the rate of pitch was varied between zero and 281° /sec. The flowfield was visually displayed by means of a multiple filament smoke technique during the flow visualization studies.

Experimental Results and Discussion

The experimental results are presented in two sections, static aerodynamics and aerodynamics while undergoing a uniform pitching motion. The static aerodynamic data provide a baseline from which the effects of pitch rate can be adjudged in terms of increments to the aerodynamic coefficients. The implications of the flow visualization studies will be incorporated into both sections.

Static Aerodynamics

Normal force, pitching moment, yaw force, and yaw moment were recorded at 5° increments of the angle of attack between zero and 90°. The test conditions were allowed to stabilize at each angle before recording the forces. Three series of experiments were conducted for nominal freestream Reynolds numbers of 5×10^4, 8×10^4, and 1.4×10^5. These Reynolds numbers were somewhat less than a critical crossflow Reynolds number of about 2×10^5, and therefore should be considered subcritical throughout the angle-of-attack range. The low-turbulence level within the wind-tunnel test section provides additional justification for assuming that the flow was subcritical for all test conditions considered.

The static aerodynamic force and moment coefficients and the center of pressure are presented in Figs. 2-4 for the three values of the freestream Reynolds number. The continuous curve represents a best fit to the experimental data for the Reynolds number 8×10^4. The magnitude of the normal force

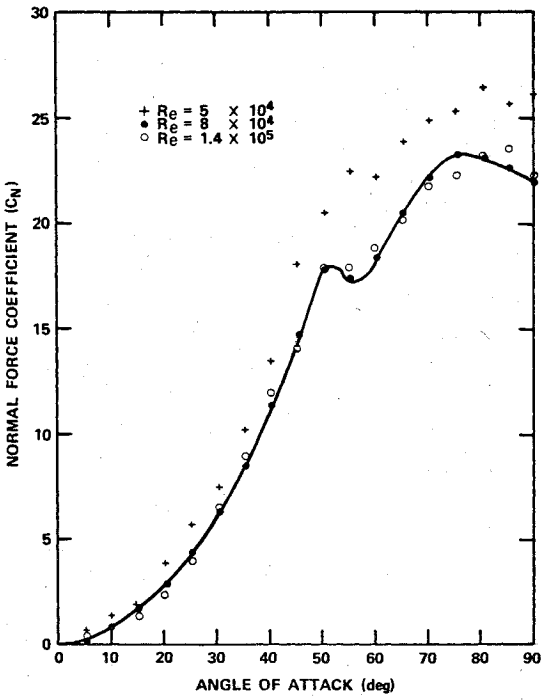

Fig. 2 Static normal force coefficient vs angle of attack for various Reynolds numbers.

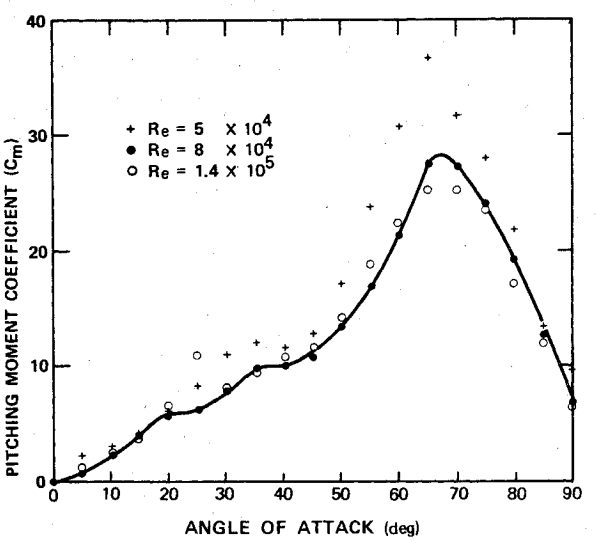

Fig. 3. Static pitching moment coefficient vs angle of attack for various Reynolds numbers.

coefficient agrees favorably with referenced data when angle of attack, length-to-diameter ratio, and Reynolds number are considered.

Reynolds Number Effects

The aerodynamic loads developed on an inclined body of revolution are strongly dependent upon the separation of boundary-layer fluid which feeds into regions of concentrated vorticity. Since the boundary-layer thickness is inversely proportional to the square root of the Reynolds number, increasing the Reynolds number decreases the boundary-layer thickness at a given position on the wall. The thinner boundary layer decreases the tendency toward separation for steady flow. Therefore, the point of separation shifts toward the leeside of the body with increasing Reynolds number as long as the flow remains laminar. As the point of separation moves farther toward the leeside of the body, the form drag (normal force) is decreased as a consequence of a greater pressure recovery on the leeside of the body. The data presented in Fig. 2 are in accordance with those arguments, showing

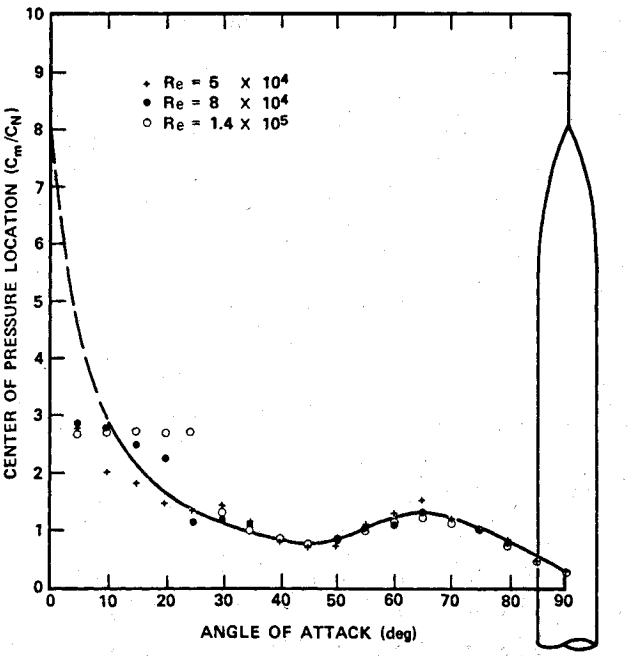

Fig. 4 Static center of pressure location vs angle of attack for various Reynolds numbers.

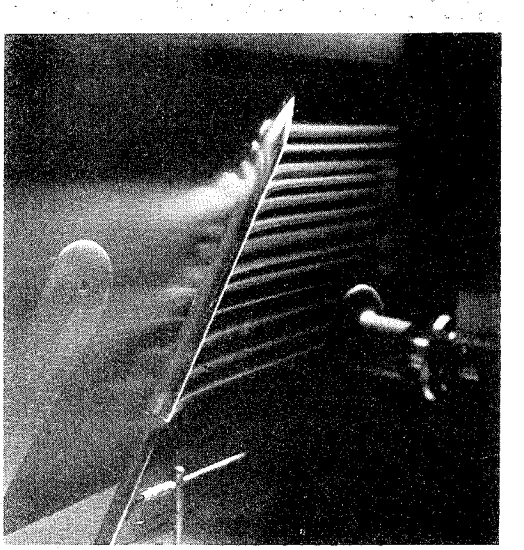

Fig. 5 Still photograph of the model at an angle of attack of 55°.

a larger normal force coefficient for a Reynolds number of 5×10^4 than for either 8×10^4 or 1.4×10^5. Considering the experimental uncertainty, the normal force coefficient at the two larger values of the Reynolds number are nearly indistinguishable, implying that the point of separation has moved a negligible amount further aft with increasing Reynolds number.

It should be noted that the Reynolds numbers under discussion are freestream values based on the maximum body diameter. The local crossflow Reynolds number will be less than the freestream value by the sine of the angle of attack for all stations along the body, and even less along the nose due to the reduced diameter. Depending upon the configuration of the wake vortices and the freestream turbulence, the separation angle can vary from approximately 80 to 110° from the front stagnation point for local Reynolds numbers between 10^3 and 10^5 which is sufficient to cause the observed result.[13]

Normal Forces

The normal force coefficient smoothly increases with increasing angle of attack between zero and about 50°. Between 50 and 60° there is an apparent stall and subsequent recovery.

Beyond this region of apparent stall, there is a loss of normal force attributed to an adjustment of the aerodynamic loads to compensate for the changing distribution of frontal area where the crossflow dominates.

The existence of the inflection in the normal force coefficient curve at about 55° was first reported by Hauer and Kelly.[14] They observed the same phenomenon for both cone/cylinders and ogive/cylinders, and attributed the inflection to flow unsteadiness during a transition from a flow dominated by the axial component to a flow in which the crossflow component dominates.

Support for this argument was obtained during the flow visualization studies. Note the persistence of the axial flow near the apex of the nose in Figs. 5-7. Also, during the pitch rate experiments, continuous normal force records show an unsteady normal force response in the region of 50-60° angle of attack.

The pitching moment curve is relatively uneventful, with the exception of some rather small deviations between about 20 and 40° angle of attack. There is no correlation between the deviations on the pitching moment curve and the inflection on the normal force curve. In the angle-of-attack range in which the deviations in the pitching moment occur, the wake can be characterized by periodic asymmetric vortex shedding. Assuming the first trailing vortex breaks away from the body at the shoulder of the nose, the spacing between trailing vortices of like sign can be calculated using the equation developed by Thomson and Morrison.[15] The spacing between trailing vortices at an angle of attack of 20° is 6.87 diam. Thus, measuring the spacing from the shoulder of the nose, one or maybe two trailing vortices would exist on the 12 diam long afterbody. At an angle of attack of 40° the spacing between trailing vortices is 2.98 diam, and at least four trailing vortices would be expected. That is, in the angle-of-attack region of periodic asymmetric vortex shedding, additional trailing vortices emanate from the base of the body with increasing angle of attack. The addition of trailing vortices at the base of the body increments the total normal force and causes a redistribution of the normal force. The incrementing of the normal force appears to be smooth, whereas the redistribution of the normal force causes the deviations in the pitching moment.

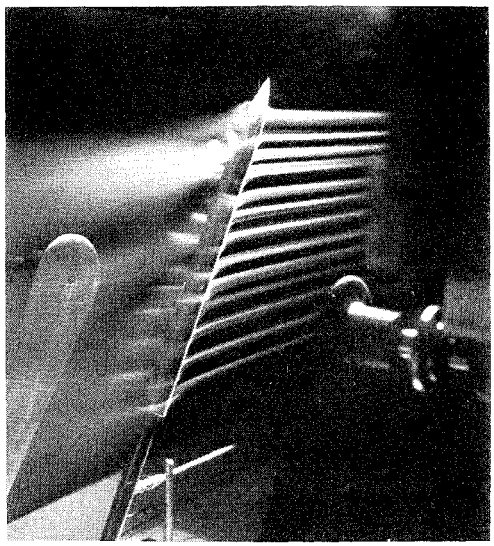

Fig. 6 Still photograph of the model at an angle of 60°.

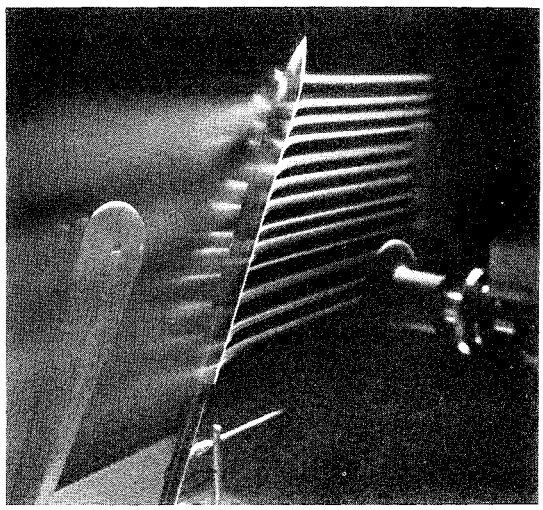

Fig. 7 Still photograph of the model at an angle of attack of 63°.

Center of Pressure Location

The scatter of the center of pressure data, presented in Fig. 4, at the low angles of attack should be disregarded since these values are obtained by dividing a small pitching moment by an even smaller normal force, and any slight error is tremendously magnified in the center of pressure location. As was to be expected, the effect of Reynolds number upon the center of pressure location was small, since the center of pressure is merely a ratio of aerodynamic loads, both of which are dependent to nearly the same extent upon the Reynolds number.

At zero angle of attack the clean axisymmetric body develops no lift. For small angles of attack the nose contributes a majority of the normal force as a result of the acceleration of the axial flow over the expanding nose. The center of pressure moves further aft from the apex with increasing angle of attack as the afterbody begins contributing more to the normal force due to the formation of wake vortices. Between 40 and 50° the center of pressure location reaches a temporary minimum, then moves forward until about 65°. As the angle of attack is further increased the center of pressure approaches a position consistent with the center of the presented frontal area at 90°. The temporary forward movement of the center of pressure indicates a loss of normal force on the aft portion of the body. This trend appears to be coupled to the inflection in the normal force curve at about 55°. As discussed earlier, the inflection is the result of a transition from a flow dominated by the axial component to a flow dominated by the crossflow component. In the region of the nose this transition is delayed until a higher angle of attack is reached so that the center of pressure moves forward. This persistence of the nose-generated vortex at high angles was dramatically illustrated during the flow visualization studies and is shown in Figs. 5-7. A curve drawn point to point in Fig. 4 would include small deviations from the smooth curve shown at angles of attack of 20 and 40° These small deviations in the center of pressure location would be the result of the similar deviations in the pitching moment.

Aerodynamics While Undergoing a Uniform Pitching Motion

The model was accelerated to the desired angular velocity from −15°, then maintained at a constant angular velocity between zero and 90°, and decelerated in another 15°. The normal force, pitching moment, yaw force, and yaw moment were continuously recorded as functions of time, as was the angle of attack. Actual pitch rates were computed from the slope of the angle of attack vs time trace.

Reynolds Number of 80,000

Pitch rate experiments were conducted at a nominal freestream Reynolds number of 8×10^4. The effects of pitch rate will be illustrated with the normal force and pitching moment coefficients.

Figure 8 shows how the normal force coefficient at various rates of pitch compares with that for the truly static case (continuous curve). Considering experimental uncertainty, it is easily seen that pitch rates of 10.8 and 21.8°/sec are not

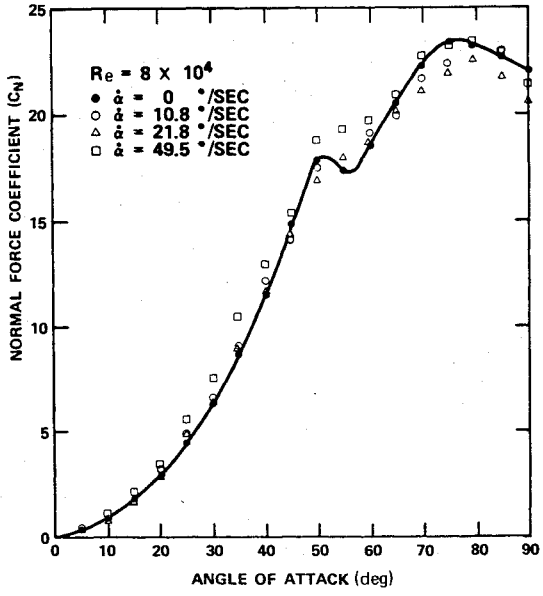

Fig. 8 Normal force coefficient vs angle of attack for various pitch rates.

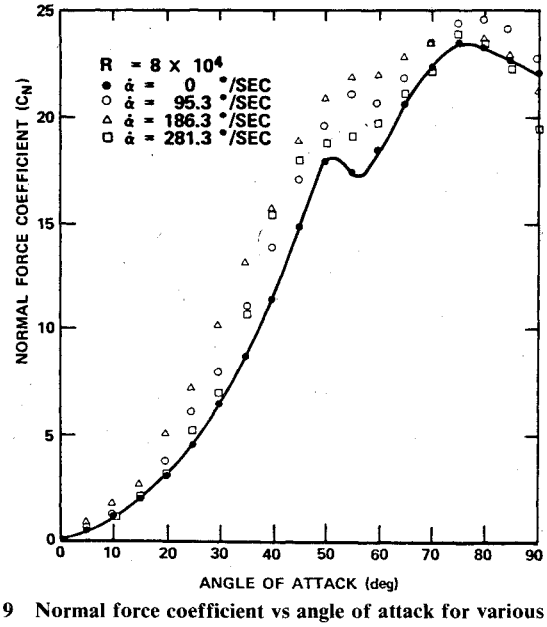

Fig. 9 Normal force coefficient vs angle of attack for various pitch rates.

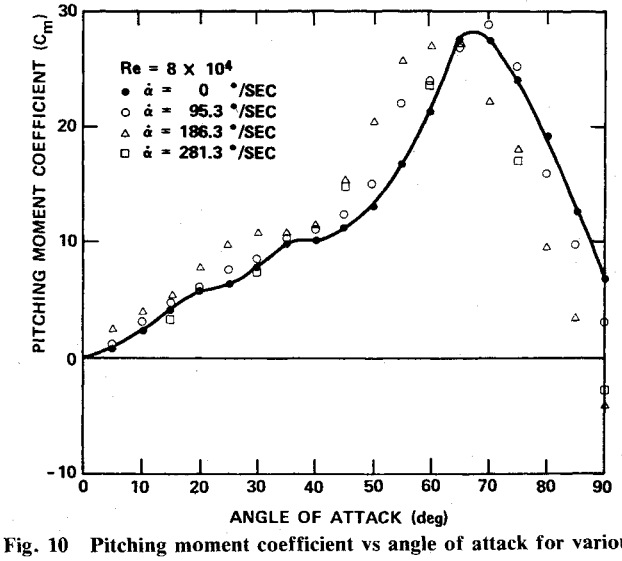

Fig. 10 Pitching moment coefficient vs angle of attack for various pitch rates.

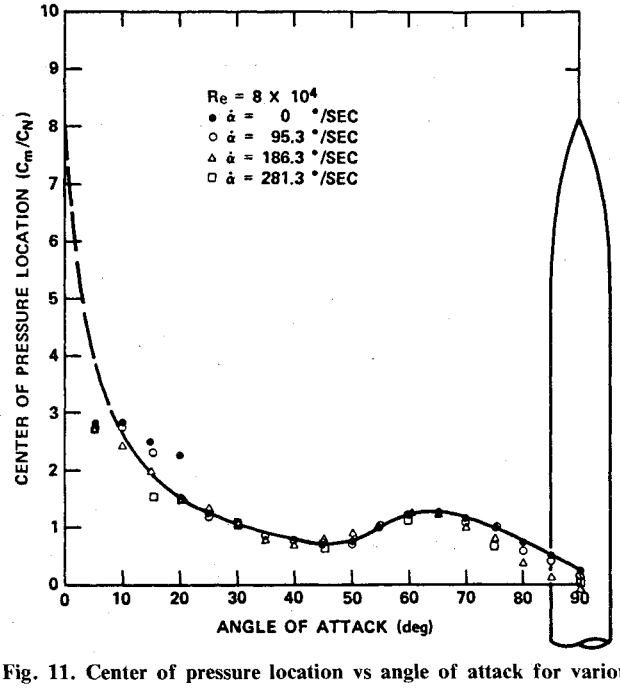

Fig. 11. Center of pressure location vs angle of attack for various pitch rates.

significantly different from the static data, at least up to 50° angle of attack. Beyond 50°, the difference may be sufficient to indicate some consistent pitch rate dependence. At an angular velocity of 49.5°/sec the normal force coefficient is fairly easily distinguished from the static data throughout the angle of attack range. A curve representing the data for this pitch rate would have a steeper slope and would reach the inflection point at a slightly higher angle of attack. The normal force coefficient is higher at the inflection and the transition appears to be more gradual than occurs in the static case. These trends were repeatable over an extensive series of corroborative tests. From Fig. 8 it can be concluded that rates of pitch less than 20°/sec are relatively indistinguishable from static data. For pitch rates greater than 20°/sec consideration must be given to the rate of pitch when interpreting the normal force coefficient.

Figure 9 compares the normal force coefficients for angular velocities of 95.3, 186.3, and 281.3°/sec with those for zero pitch rate. The trends established for 49.5°/sec are supportcd by the data for 95.3 and 186.3°/sec; that is, an increasing coefficient magnitude at a given angle of attack and a shifting of the angle at which the inflection occurs. However, with a further increase in the angular velocity to 281.3°/sec the coefficient magnitude decreases, and the angle at which the inflection occurs nearly returns to the value for the static case. A discussion of this trend reversal will be delayed until a constant pitch rate parameter is discussed.

Figure 10 shows the pitching moment coefficient for the same angular velocities. The maximum value of the pitching moment coefficients and the general shape of the curves remain relatively independent of pitch rate, although the angle of attack at which the maximum occurs decreases with increasing pitch rate. Again, at 281.3°/sec the trend is reversed.

The center of pressure curve, presented in Fig. 11, illustrates the similarity of the normal force and pitching moment curves at the various rates of pitch to those for zero pitch rate. The data for nonzero pitch rates falls on essentially the same curve as the static data up to about 75°. The divergence of the data above an angle of 75°indicates a more rapid adjustment of the normal force to the distribution of the frontal area with increasing rates of pitch. The more rapid ad-

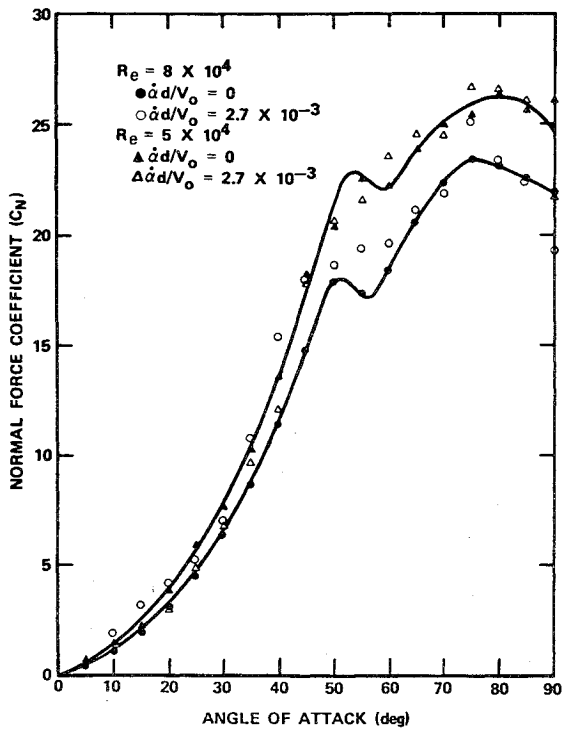

Fig. 12. Normal force coefficient vs angle of attack for various Reynolds numbers at a constant value of the pitch rate parameter.

justment with increased pitch rate is also apparent in Fig. 10, where the pitching moment decays more rapidly for the higher pitch rates. These results may be a consequence of the experimental setup; that is, in these experiments the center of the frontal area presented at an angle of attack of 90° coincides with the axis of rotation. Referring to Figs. 8 and 9, the normal force coefficients for all pitch rates converge on the static value for angles of attack above about 75°. Therefore, it is suggested that pitch rate effects apparent in these data above an angle of attack of 75° are, in fact, a consequence of the particular experimental setup.

Constant Pitch Rate Parameter

A second sequence of experiments was conducted to determine if the Reynolds number effects at a constant value of the pitch rate parameter, $\dot{\alpha}d/V_0$, would be consistent with the pitch rate trends established at a Reynolds number of 8×10^4. Experiments were conducted for a value of the pitch rate parameter of 2.7×10^{-3} for Reynolds numbers of 5×10^4 and 8×10^4. The normal force coefficients obtained during these experiments are presented in Fig. 12. A comparison of the continuous curves for zero pitch rate and the data points for the same nonzero pitch rate are consistent. That is, the normal force coefficient at the lower Reynolds number is greater than the normal force coefficient for the higher Reynolds number for both a zero and a nonzero pitch rate. Further examination of Fig. 12 illustrates the insensitivity of the normal force to pitch rate at a Reynolds number of 5×10^4. However, the data indicate that increasing pitch rate may have an overall effect of decreasing the freestream Reynolds number, at least at the lower angles of attack. That is, at low angles of attack, the data for $\dot{\alpha}d/V_0 = 2.7\times10^{-3}$ and $R_e = 8\times10^4$ (the open circles in Fig. 12) appear to fall on the $R_e = 5\times10^4$ curve. The effect of pitch rate is to decrease the local crossflow velocity on that portion of the body forward of the axis of rotation while increasing the crossflow velocity aft of the axis of rotation. Although for the angular velocities investigated the maximum change in velocity induced by pitch rate was less than 3 ft/sec, the net effect is to reduce or disturb the crossflow Reynolds number near the apex where the wake vortex configuration is established for the entire body. This disturbance of the crossflow Reynolds number on the nose appears to cause an increase in the normal force for low angles of attack where the axial flow dominates. In other words, even though the freestream Reynolds number is constant, the local crossflow Reynolds number is affected by the rate of pitch. This description seems to be valid only if the freestream Reynolds number is such that the increment of velocity due to pitch causes some change in the flow state, at a station where the local flow conditions control a large portion of the flowfield about the remainder of the body.

Conclusions

The results of this experimental investigation serve to establish baseline static aerodynamic data for a particular configuration and to illustrate the influence of a constant rate of pitch upon the aerodynamic loads for large excursions in angle of attack. In addition, flow transitions within the wake vortex system were observed during the flow visualization studies and correlated with observed changes in the force and moment coefficients. The results presented herein, although not directly applicable to the design of a missile airframe, do provide additional insight into some of the potential flow anomalies that may occur during an actual flight or during wind-tunnel tests.

The results of this investigation show that there is an increment of normal force directly attributable to the uniform pitching motion. While undergoing uniform pitching, the normal force curve has a steeper slope, reaches the inflection point at a slightly higher angle of attack, and the inflection is less abrupt. The increment of normal force caused by uniform pitching is closely coupled to the Reynolds number, and may only be apparent if the angular velocity induces a local velocity increment at a station where the crossflow Reynolds number would otherwise remain at a threshold to some change in the separation angle, boundary layer transition point, or change in the wake vortex configuration.

It was observed that for pitch rates of less than 20°/sec the normal force curve is not significantly different from the static case at least up to about 50° angle of attack. Beyond 50°, the difference may be sufficient to indicate some consistent pitch rate dependence. It must be cautioned that these results were obtained while pitching the body about a point which nearly coincides with the center of the frontal area. The identification of a maximum pitch rate at which a body can be rotated, such that the normal force is still essentially that for the static case, must include a definition of where the axis of rotation is located. That is, it appears possible to rotate a body about an axis such that the increment of normal force due to constant angular velocity could be nullified.

References

[1] Allen, H.J. and Perkins, E.W., "Characteristics of Flow Over Inclined Bodies of Revolution," NACA RM A50L07, Jan. 1951.

[2] Allen, H.J. and Perkins, E.W., "A Study of Effects of Viscosity on Flow Over Slender Inclined Bodies of Revolution," NACA Rept. 1048, 1951.

[3] Kelly, H.R., "The Estimation of Normal-Force, Drag, and Pitching-Moment Coefficients for Blunt-Based Bodies of Revolution at Large Angles of Attack," *Journal of the Aeronautical Sciences*, Vol. 21, Aug. 1954, pp. 549-565.

[4] Jorgensen, L.H. "Prediction of Static Aerodynamic Characteristics for Space-Shuttle-Like and Other Bodies at Angles of Attack From 0° to 90°," NASA TN D 6996, Jan. 1973.

[5] Thomson, K.D., "The Estimation of Viscous Normal Force, Pitching Moment, Side Force and Yawing Moment on Bodies of Revolution at Incidences Up to 90°," Rept. 782, Oct. 1972, Weapons Research Establishment, Salisbury, South Australia.

[6] Bryson, A.E., "Symmetric Vortex Separation on Circular Cylinders and Cones," *Journal of Applied Mechanics*, Vol. 26, pp. 643-648 Dec. 1959

[7] Sarpkaya, T., "Separated Flow About Lifting Bodies and Impulsive Flow About Cylinders," *AIAA Journal*, Vol. 4, March 1966, pp. 414-420.

[8] Schindel, L.H., "Effects of Vortex Separation on the Lift Distribution on Bodies of Elliptic Cross Section," *Journal of Aircraft*, Vol. 6, Nov.-Dec. 1969, pp. 537-543.

[9] Angelucci, S.B., "A Multivortex Method for Axisymmetric Bodies of Angle of Attack," *Journal of Aircraft*, Vol. 8, Dec. 1971. pp. 959-966.

[10] Wardlaw, A.B., "Prediction of Normal Force, Pitching Moment, and Yawing Forces on Bodies of Revolution at Angles of Attack Up to 50 Degrees Using a Concentrated Vortex Flow-Field Model," Rept. 72-209, Oct. 1973, Naval Ordnance Lab., White Oak, Md.

[11] Sarpkaya, T., "Separated Unsteady Flow About a Rotating Plate," *Developments in Mechanics*, Vol. 4, 1968, pp. 1485-1499.

[12] Glauert, H., "The Lift and Pitching Moment on an Aerofoil Due to a Uniform Angular Velocity of Pitch," R&M 1216, Nov. 1928, Aeronautical Research Council London, pp. 636-646.

[13] Coder, D.W., "Location of Separation on a Circular Cylinder in Crossflow as a Function of Reynolds Number," Rept. 3647, Nov. 1971, Naval Ship Res. and Devl. Center, Bethesda, Md.

[14] Hauer, H.J. and Kelly, H.R., "The Subsonic Aerodynamic Characteristics of Spinning Cone-Cylinders and Ogive-Cylinders at Large Angles of Attack," Rept. 3529 (NOTS 1166), July 1955, Naval Ord. Test Sta., China Lake, Calif.

[15] Thomson, K.D. and Morrison, D.F., "The Spacing, Position and Strength of Vortices in the Wake of Slender Bodies at Large Incidence," *Journal of Fluid Mechanics*, Vol. 50, Dec. 1971, pp. 751-783.